Magnetic Resonance in Medicine 52:19–26 (2004)

Accelerating Cardiac Cine 3D Imaging Using *k-t* BLAST

Sebastian Kozerke,[1,2*] Jeffrey Tsao,[2] Reza Razavi,[1] and Peter Boesiger[2]

By exploiting spatiotemporal correlations in cardiac acquisitions using *k-t* BLAST, gated cine 3D acquisitions of the heart were accelerated by a net factor of 4.3, making single breathhold acquisitions possible. Sparse sampling of *k-t* space along a sheared grid pattern was implemented into a cine 3D SSFP sequence. The acquisition of low-resolution training data, which was required to resolve aliasing in the *k-t* BLAST method, was either interleaved into the sampling process or obtained in a separate prescan to allow for shorter breathhold durations in patients with heart disease. Volumetric datasets covering the heart with 20 slices at a spatial resolution of $2 \times 2 \times 5$ mm^3 were recorded with 20 cardiac phases in a total breathhold duration of 25–27 sec, or 18 sec if partial Fourier sampling was additionally employed. The feasibility of the method was demonstrated on healthy volunteers and on patients. The comparison of endocardial area derived from single slices of the 3D dataset with values extracted from separate single-slice acquisitions showed no significant differences. By shortening the acquisition substantially, *k-t* BLAST may greatly facilitate volumetric imaging of the heart for evaluation of regional wall motion and the assessment of ventricular volume and ejection fraction. Magn Reson Med 52:19–26, 2004. © 2004 Wiley-Liss, Inc.

Key words: cardiac imaging; prior knowledge; reduced acquisition; *k-t* BLAST

Recent advances in scanner hardware and sequence design have made multislice, multibreathhold imaging based on steady-state free precession (SSFP) the method of choice for obtaining cine views of the heart. From these images, functional parameters can be determined with high accuracy and reproducibility (1–3). There are, however, limitations associated with multislice, multibreathhold acquisitions. Inconsistencies in the multiple breathholds may lead to misregistration of slices. Furthermore, the low bandwidth-time product of the excitation pulses used for short TR SSFP imaging results in large variations of excitation angles within the slice. This not only affects the signal-to-noise and contrast-to-noise ratios (SNR, CNR), it also hampers the reconstruction of multiplanar reformats through the heart due to the slab boundary artifact. Cine 3D SSFP imaging of the heart has already been shown to offer superior SNR and CNR (4). However, compromises in image quality and spatial and temporal resolutions had to be made to accommodate sufficient volume coverage into a single breathhold. Using an elliptical shutter in k_y-k_z space, cine volumetric datasets may be obtained at relatively high spatial resolution in a single breathhold (4). Still, temporal sampling does not satisfy the requirements for accurate left ventricular volume calculations. Generally, at least 10 temporal frequency harmonics are considered sufficient for accurate volume curve calculation, requiring a sampling rate of at least $20 \times$ HR/60 Hz, with HR being the actual heart rate (5).

The high intrinsic SNR and CNR of SSFP imaging make it a good candidate for reduced data acquisition schemes. Sparse sampling of *k*-space may allow shortening of scan time. At the same time, shorter scan time has the added benefit of reducing the overall power deposited in the subject, which is a concern for cardiac SSFP imaging, especially at higher field strengths.

Several methods for accelerating image acquisition have been described. In parallel imaging such as the SENSitivity Encoding (SENSE) method, effects of spatial undersampling are corrected by means of distinct sensitivities of multiple receive coils (6). Since reconstruction is applied on a frame-by-frame basis, it does not take the temporal dimension into account. Alternatively, cine image acquisitions may be accelerated by a factor of two without the need for multiple receive channels using the UNaliasing by Fourier-encoding the Overlaps using the temporaL Dimension (UNFOLD) method (7). UNFOLD may be combined with parallel imaging to reduce susceptibility to image artifacts (8) or to achieve acceleration factors greater than two by repopulating missing data using information from multiple coils (9).

More recently, an approach for accelerated data acquisition in dynamic imaging has been reported, called Broad-use Linear Acquisition Speed-up Technique (BLAST), which allows acceleration factors greater than two for single coil applications (10). An extension of this method, called *k-t* BLAST (11), applies sparse sampling to *k-t* space (k = wavenumber, t = time), thus leading to dense packing of signal replicas in the reciprocal *x-f* space (x = spatial position, f = temporal frequency). Potential signal aliasing is resolved using signal correlations learned from low-resolution training data.

The main objective of the current work was to apply *k-t* BLAST to cardiac-gated volumetric cine acquisition of the heart for scan time reduction. In general, each new application of *k-t* BLAST requires careful consideration, since the performance of this method depends on the signal distribution in *x-f* space, and is therefore content-dependent (11). This particular application of 3D cardiac cine imaging poses both challenges and favorable opportunities. The key challenge is that the *k-t* concept is applied to the pseudo-time axis, which refers to cardiac phases acquired with cardiac gating rather than real-time imaging

[1]Department of Imaging Sciences, Guy's Hospital, King's College, London, UK.

[2]Institute for Biomedical Engineering, University and ETH Zurich, Zurich, Switzerland.

Grant sponsors:Philips Medical Systems, Best, NL, UK EPSRC-MRC Medical Images and Signals Interdisciplinary Research Collaboration (to S.K.), Canadian Institutes of Health Research (CIHR) (postdoctoral fellowship to J.T.), EUREKA and the Swiss Commission for Technology and Innovation; Grant numbers: E12061; 4178.1, INCA-MRI.

*Correspondence to: Sebastian Kozerke, Institute for Biomedical Engineering, University and ETH Zurich, Gloriastrasse 35, 8092 Zurich, Switzerland. E-mail: kozerke@biomed.ee.ethz.ch

Received 21 August 2003; revised 8 March 2004; accepted 10 March 2004.

DOI 10.1002/mrm.20145

Published online in Wiley InterScience (www.interscience.wiley.com).

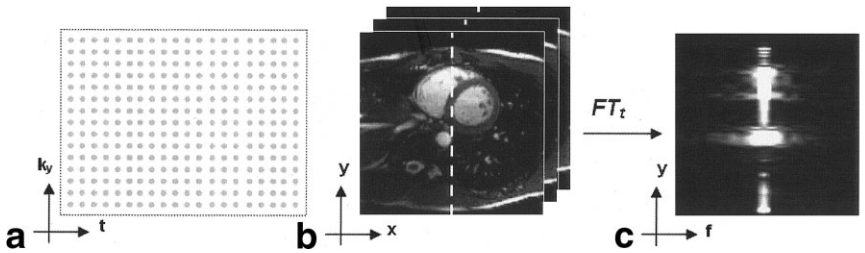

FIG. 1. Regular sampling (**a**), resulting time series (**b**) and corresponding signal distribution of object intensities along dashed line in (**b**) after inverse Fourier transform over time (**c**).

presented previously (11). Since the number of cardiac phases is usually limited, this restricts the dimension of the *f* axis in *x-f* space, potentially leading to increased signal crowding. On the other hand, the use of 3D imaging introduces an additional spatial axis (compared to 2D imaging), which provides significantly more room in *x-f* space. The extra axis also enables the incorporation of *k*-space shutters for further reduction of scan time. The present investigation shows that for the typical image contents observed in 3D cine cardiac imaging, it is indeed feasible to accelerate the acquisition with *k-t* BLAST. A net acceleration of 4.3 is achieved on healthy volunteers and cardiac patients. Methodologically, two developments are introduced. First, a single breathhold sampling strategy is proposed, allowing the interleaved acquisition of the low-resolution training data necessary in the *k-t* BLAST method. This enables the entire dataset to be acquired in a single scan, albeit at the expense of a longer breathhold. Second, it is shown that *k-t* BLAST can be used with multiple receiver coils by applying the coil-by-coil reconstruction concept (12).

MATERIALS AND METHODS

In the following a brief review of the *k-t* BLAST method is given. A detailed description of the method and its connection to related methods can be found in Ref. 11 and references therein. Image content in a cine series of the heart exhibits a high degree of correlation in both space and time. This is demonstrated in Fig. 1, showing a fully sampled, cine short-axis acquisition of the heart. Image information along a vertical profile through the heart (Fig. 1b) is confined to compact regions in *x-f* space, according to the dynamics of the corresponding image pixels (Fig. 1c). In the *k-t* BLAST method, acquisition efficiency is increased by applying sparse sampling to *k-t* space according to a sheared grid pattern, resulting in tighter packing of signal replica in the reciprocal *x-f* space. Using low-resolution image information sampled for all cardiac phases (Fig. 2a), an estimate of the expected signal distribution in *x-f* space is obtained, which is used to determine a reconstruction filter (Fig. 2b). The sparse sampling in the actual, high-resolution acquisition results in multiple replica in *x-f* space, which in turn manifest as multiple fold-over in the actual image series (Fig. 2c). By multiplying the acquired, high-resolution data with the reconstruction filter, an unfolded image series is obtained (Fig. 2d). This unfolding process deserves further explanation. As Fig. 2c shows, each voxel in the aliased *x-f* space holds the signals originating from multiple *x-f* locations. In the case of 5× acceleration, the signals from five *x-f* locations are mapped (i.e., aliased) onto a single location. Due to the undersampling, there is insufficient information to completely resolve the signals originating from the respective locations. Nevertheless, there are enough data to recover at least one degree of freedom for each set of aliased *x-f* voxels. This single degree of freedom can be shared among the aliased voxels, as long as the relationship among their signals can be estimated. Using the parlance from statistics, it is possible to recover one mode of variation for each set of aliased voxels. It is precisely the function of the reconstruction filter (Fig. 2b) to distribute this degree of freedom in a manner that minimizes the expected reconstruction error, as described in Ref. 11. A key purpose of the current work was to investigate if the correlations learned from the training data were sufficient to provide adequate signal separation for volumetric cine cardiac images.

As shown in the outline in Fig. 2, designing a *k-t* BLAST experiment involves two steps. First, for data acquisition a sampling pattern needs to be implemented to allow for

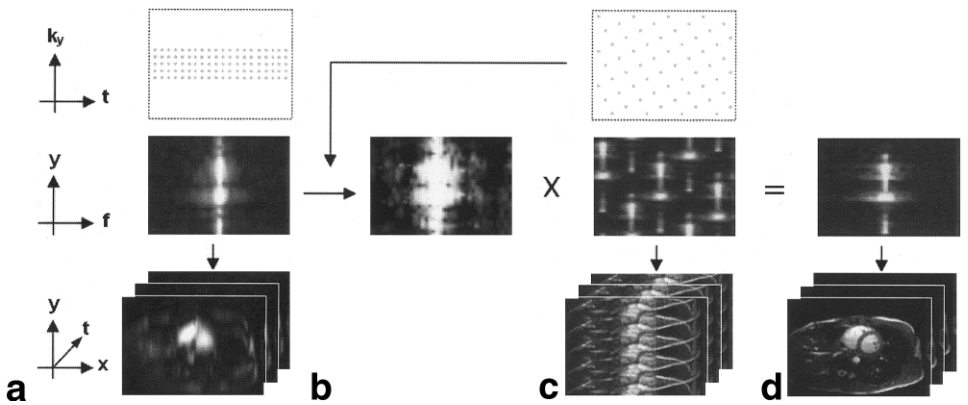

FIG. 2. Schematics of the *k-t* BLAST method. Using low-resolution, fully sampled data (**a**) an estimate of the expected signal intensities in *x-f* space (y-f space in this example) is used to determine the reconstruction filter (**b**). The fold-over apparent in the high-resolution data (**c**) is removed by applying the determined filter. After Fourier transform along the time axis, an unfolded images series is obtained (**d**).

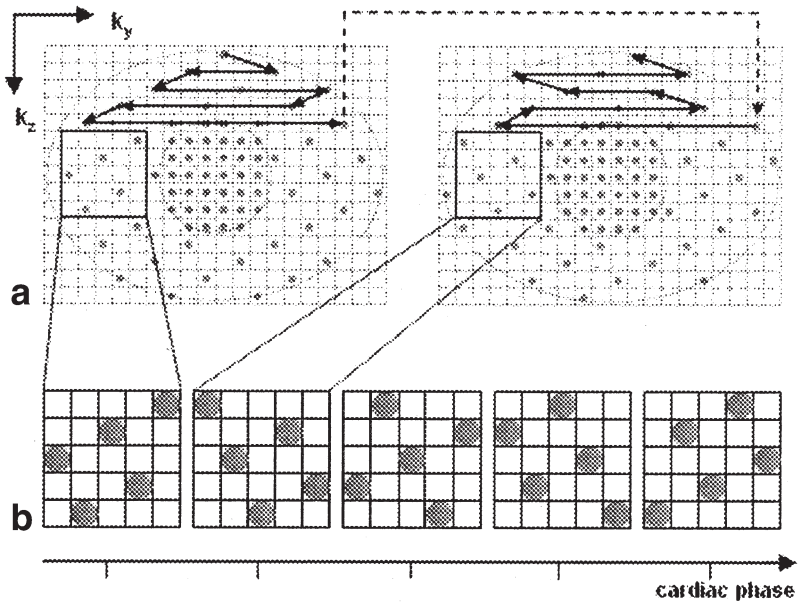

FIG. 3. Sampling pattern for cine 3D *k-t* BLAST. The central portion of ky-kz space is sampled at the full FOV in each cardiac phase, whereas the outer portion is subsampled by a factor of five with the pattern being shifted as a function of cardiac phase (gray dots indicate sampled points). The *k*-space trajectory is indicated (black arrows) and the elliptical shutters applied are shown (**a**). The fundamental sampling tile for 5-fold acceleration is given for five consecutive cardiac frames (**b**). Greater numbers of cardiac frames or *k*-space profiles can be composed by replication of the fundamental tiles.

tightest packing in *x-f* space without or with minimal signal overlap. Second, for image reconstruction a reconstruction filter is derived from low-resolution, fully sampled data to account for the expected signal distribution in *x-f* space.

Data Acquisition

Sampling along a sheared grid pattern was implemented into the acquisition software of a Philips Gyroscan Intera system (Philips Medical Systems, Best, The Netherlands). Subjects were placed in supine position and a five-element cardiac phased array coil was wrapped around the subject's chest. A vector electrocardiograph (ECG) was connect for cardiac gating (13).

As indicated in Fig. 3a, an elliptical *k*-space shutter was applied to reduce the number of points to be sampled by ~25%. The *k*-space shutters were applied to both the acquisition of the undersampled, high-resolution data and the acquisition of the low-resolution training data. To reduce eddy current-related distortions induced by the changing phase-encoding gradients, a modified profile order was implemented. Consecutive profiles in the k_y-k_z plane are traversed in a contiguous fashion, with the overall direction of sampling being reversed for odd cardiac phases (Fig. 3a). This scheme has been shown to reduce eddy current-related distortions by ensuring maximum compensation of phase-encode gradient lobes (4).

For each of five consecutive cardiac phases, a shifted version of the undersampled sheared grid pattern is acquired. The undersampled pattern can be generated by duplication of the fundamental tile, as shown in Fig. 3b.

Using 5-fold undersampling (5× *k-t* BLAST), volumetric datasets covering the heart with 20 slices at a spatial resolution of $2 \times 2 \times 5$ mm^3 were recorded with 20 cardiac phases in a single breathhold of 20–22 sec. with the training data acquired in a separate 5-sec prescan. This will be referred to as split acquisition. When the training data were acquired together with the undersampled data in a single scan (referred to as interleaved acquisition hereafter), the breathhold duration was prolonged slightly to 25–27 sec. For interleaved acquisition, positions in the k_y-k_z plane were sampled along the *k*-space trajectory, as shown in Fig. 3a. The central, densely sampled region in the k_y-k_z plane consisted of 49 profiles providing low-resolution images without aliasing. For split acquisition, the central, densely sampled portion was acquired in a short prescan. All positions in the k_y-k_z plane coinciding with the sheared grid pattern (Fig. 3a) were acquired in a second breathhold thereafter.

Remaining acquisition parameters were as follows: FOV: 320×210 mm^2, TE/TR: 1.55/3.1 ms, flip angle: 45°, heart phase interval: 28–37 ms. Taking the acquisition of low-resolution training data into account, the net acceleration factor was 4.3.

Navigator-based volume tracking (14) was implemented in order to ensure consistency between the low-resolution, fully sampled data and the high-resolution, undersampled data when the two datasets were acquired in separate acquisitions. Using pencil-beam excitation on the diaphragm, the navigator signal corresponding to the breathhold position in the first acquisition was recorded and correlated with a navigator acquired prior to the second acquisition. Volume tracking was applied to account for possible shifts in breathhold positions. A constant tracking factor of 0.8 was applied to correlate diaphragm and cardiac motion. Accordingly, the volume position was adapted for different respiratory positions during separate breathholds. To assess the accuracy of the two consecutive breathholds, diaphragm positions as detected by the navigators were recorded into a file and absolute differences of breathhold positions between the undersampled and training acquisitions were calculated thereafter.

Image Reconstruction

The data were divided into two sets for reconstruction: a training set (Fig. 2a) and an undersampled set (Fig. 2c).

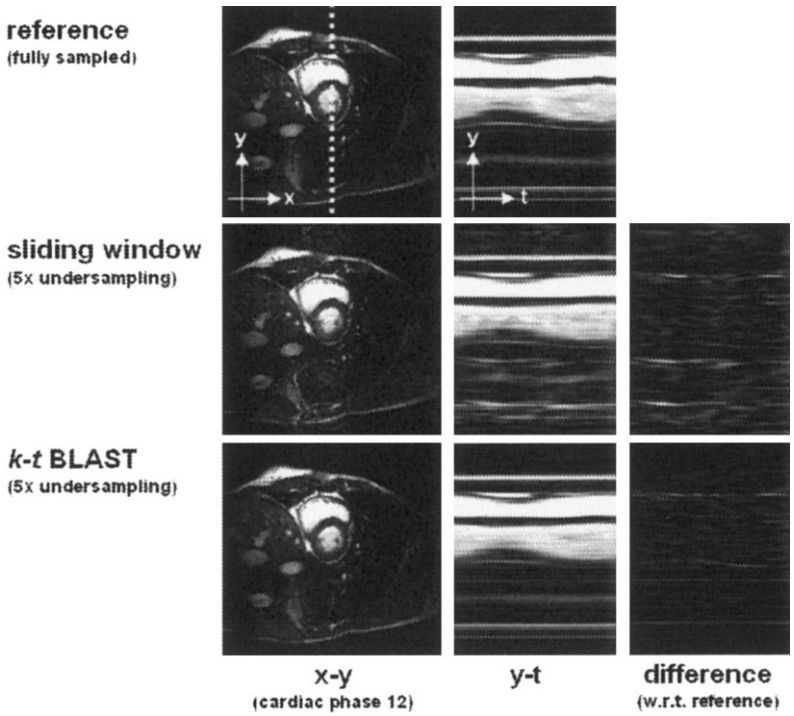

FIG. 4. Simulation results. Short axis images acquired during rapid motion of the heart (left column) are shown along with a depiction of the temporal changes along a long-axis cut (dashed line) through the heart (middle column). The fully sampled dataset (reference) was decimated by a factor of five according to the sampling pattern indicated in Fig. 3. Resulting images from sliding window reconstruction (middle row) and *k-t* BLAST reconstruction (lower row) are shown along with the difference images with respect to the reference dataset. All images are scaled identically.

The training set consisted of the densely sampled central region of *k*-space only, while the undersampled set consisted of all the data sampled along the sheared grid pattern. Both datasets were inverse Fourier transformed along all axes. The training set yielded a set of low-resolution images in *x-f* space, while the undersampled set yielded a set of aliased images in *x-f* space. For each set of aliased voxels in *x-f* space, the aliasing was resolved by the following equation:

$$p = \lfloor \Theta E^H (E\Theta E^H + \Psi)^{-1} \rfloor a. \quad [1]$$

Vector p represents the reconstructed (unaliased) intensities. Θ is a diagonal matrix, with the diagonal elements representing the squared expected intensities, as determined from the training data. E denotes the encoding matrix, representing the process of aliasing. Ψ is the noise variance of the acquisition data. Vector a holds the aliased intensity of the voxels. The time-averaged signals of the object were subtracted prior to reconstruction. After reconstruction, the object corresponding to the time-invariant signals was added back. The rationale for the treatment of the time-invariant signals is described in Ref. 11. The square-bracketed portion corresponds to the reconstruction filter, as shown in Fig. 2b.

The training data were substituted into the reconstructed image for improved data consistency, if the training data were acquired in an interleaved fashion. To reduce computation, reconstruction was performed separately for each coil element and the reconstructed images were combined afterwards as the root-mean-square of the coil images.

Reconstruction software was written in C and implemented on a separate PC station. Image reconstruction for a dataset consisting of 20 slices, 20 cardiac phases, and five coils takes ~1 min, excluding time needed for data transfer. The additional time for data transfer will become unnecessary as soon the reconstruction software is fully integrated on the system.

Computer Simulations

To validate the performance of the *k-t* BLAST method with respect to reconstruction accuracy, a fully sampled cine 2D cardiac dataset acquired in the short-axis orientation in a healthy volunteer was used and subsequently decimated to simulate reduced data acquisition. Figure 4 shows short axis views at late systole acquired during rapid motion of the heart along with spatiotemporal plots of a profile through the heart chamber. Figure 4 (upper row) displays images reconstructed from fully sampled data (reference). Undersampled data acquisition was simulated by decimating the original data in the Fourier domain by a factor of 5 according to the sheared sampling pattern indicated in Fig. 3.

Two different methods of reconstruction were applied to generate images from the undersampled data. First, sliding window reconstruction using a boxcar kernel was used (15). Given 5-fold undersampling of the original data, the width of the sliding window encompassed five consecutive phases. For each cardiac phase an image was reconstructed. Time frames were wrapped at the beginning and at the end of the cardiac cycle. Resulting images are shown in Fig. 4 (middle row) along with the absolute difference of the spatiotemporal plot with respect to the fully sampled reference data.

The second reconstruction employed the *k-t* BLAST method. The training dataset consisted of nine profiles. Resulting images and absolute difference maps are given in Fig. 4 (lower row). It is seen that *k-t* BLAST reconstruc-

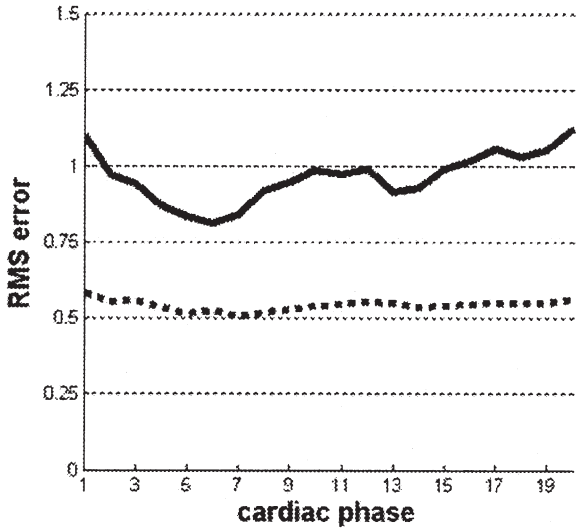

FIG. 5 Simulation results. Comparison of the RMS error of sliding window reconstruction (solid line) with *k-t* BLAST reconstruction (dashed line) as function of time within the cardiac cycle.

tion results in superior image quality, with good preservation of image features even at points in the cardiac cycle with rapid motion of the heart.

Reconstruction accuracy as a function of time was assessed by calculating the average root-mean-square error with respect to the reference data for each time frame. It is seen from Fig. 5 that the error with sliding window reconstruction is about two times the error found in the image series reconstructed with the *k-t* BLAST method.

A second set of simulations based on the fully sampled in vivo data was carried out to determine the number of training profiles needed to achieve a given reconstruction accuracy.

The absolute reconstruction error across the heart was assessed for different amounts of training data. Additionally, left ventricular contours were automatically extracted using threshold-based segmentation.

For 5-fold acceleration, results revealed that the acquisition of nine profiles is sufficient to keep the absolute reconstruction error below 5% across the heart. The absolute difference of contour area averaged over the cardiac cycle obtained from decimated data reconstructed with nine training profiles and full data was 2.30 ± 2.32% (mean ± SD). For comparison, intraobserver variability of contour detection as assessed in one subject was 3.20 ± 3.71%.

Compared to 2D imaging, the relative amount of training profiles in 3D imaging can be reduced further by skipping the corners of the k_y-k_z sampling plane using an elliptical *k*-space shutter. Accordingly, the number of training profiles to acquire was decreased to 49 in 3D imaging.

In Vivo Validation

The study population consisted of four healthy volunteers and four patients undergoing cardiac MR imaging for assessment of congenital heart disease. An additional dataset was acquired in one patient using 65% partial Fourier sampling along the k_y phase-encode direction in conjunction with the *k-t* BLAST method to reduce the breathhold duration further. For this exemplary scan, both the undersampled acquisition and the acquisition of training data were obtained in a single breathhold of 18 sec duration. In all healthy subjects, training data were interleaved into the acquisition process, resulting in single-breathhold acquisitions. In four out of the five patients, the acquisition of training data was obtained in a separate prescan to allow for shorter breathhold durations during the acquisition of undersampled, high-resolution data. In both study groups, conventional, multislice 2D SSFP acquisitions were obtained additionally for comparison, which required 9 sec per slice. Each slice was acquired in a separate single breathhold with imaging parameters comparable to the single-breathhold 3D *k-t* BLAST acquisition. Left ventricular contours were extracted using standard postprocessing software, and the contour area from the single-slice and 3D acquisitions was compared by calculating the absolute difference in area and subsequent averaging of the difference error for all measured phases.

RESULTS

In all subjects, 3D datasets were successfully acquired. Nearly artifact-free 3D volumes were reconstructed, allowing reformatting along arbitrary views.

The split acquisitions as applied in four patients were tolerated well, with good consistencies of the breathhold levels of the two scans. The mean absolute difference of the two consecutive breathholds as measured by the respiratory navigators on the left hemidiaphragm was 3.4 ± 2.9 mm. Slight image ghosting remained from residual eddy current effects. In two healthy subjects with large variations of the R-R interval during the breathhold, early diastolic frames exhibited a small degree of blurring. Image blurring, however, did not extend into image frames at time points of rapid cardiac motion during the cardiac cycle.

In Fig. 6a, the central 15 slices at end systole of a 5× *k-t* BLAST acquisition obtained in a healthy subject are shown. Figure 6b depicts selected time frames of a midventricular short-axis slice, along with reformatted four-chamber views. Figure 7 shows example images obtained from one of the patients who had repaired Tetralogy of Fallot and pulmonary regurgitation causing right ventricular dilation. In four of the five patients, training data were obtained in a separate prescan, lasting 5 sec, in order to allow shorter breathhold durations of the high-resolution 3D acquisition. In in vivo validation, the mean absolute difference of left ventricular contours extracted in three exemplary slices of the 3D dataset and the multislice 2D acquisition was 3.45 ± 6.58%.

By using partial Fourier sampling in conjunction with *k-t* BLAST, scan duration can be reduced to 18 sec, allowing for single breathhold acquisitions even in patients, as demonstrated in Fig. 8. The use of *k-t* SENSE may also lead to improved reconstruction accuracy and allow higher acceleration, albeit at the expense of increased computational effort (11). This will be investigated in the future.

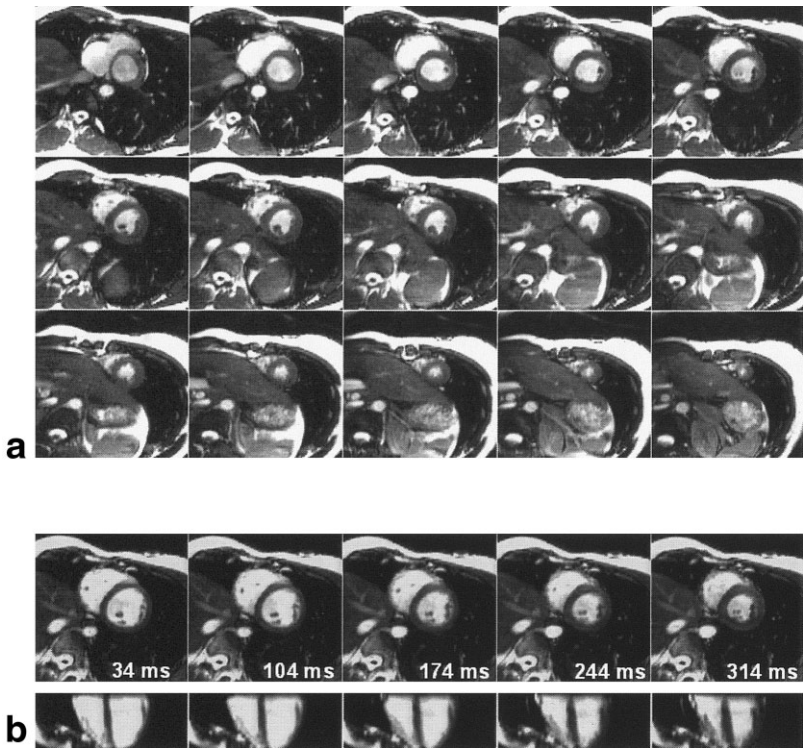

FIG. 6. Cine 3D single breathhold dataset obtained with 5× *k-t* BLAST in a volunteer. The central 15 slices are shown for the end-systolic phase (**a**). Selected time frames showing both short-axis and reformatted four-chamber view plane (**b**) (20 time-frames were sampled every 35 ms in a single breathhold of 25 sec).

DISCUSSION AND CONCLUSION

In this work, *k-t* BLAST was successfully extended from 2D real-time acquisition, as presented previously, to gated, cine 3D acquisition of the heart. It is shown that the *k-t* BLAST scheme is applicable to datasets in pseudo-time, which refers to data acquisitions employing cardiac gating. In cardiac-gated acquisitions, only a small number of cardiac phases is sampled. This leads to denser signal packing in *x-f* space compared to a real-time image series covering a larger number of time frames. Thus, the reconstruction error is expected to be larger than that for a comparable real-time acquisition. On the other hand, the

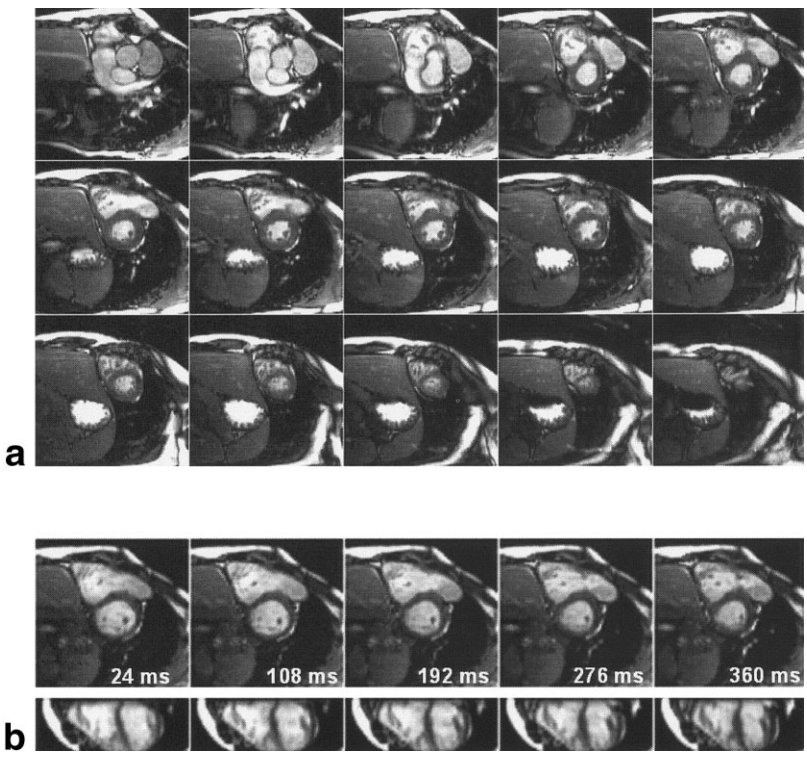

FIG. 7. Cine 3D single breathhold dataset obtained with 5× *k-t* BLAST in a patient with repaired Tetralogy of Fallot and pulmonary regurgitation causing right ventricular dilation. The central 15 slices are shown for the end-systolic phase (**a**). Selected time frames showing both short-axis and reformatted four-chamber view planes (**b**) (25 time-frames were sampled every 28 ms in two breathholds of 20 sec and 5 sec, respectively).

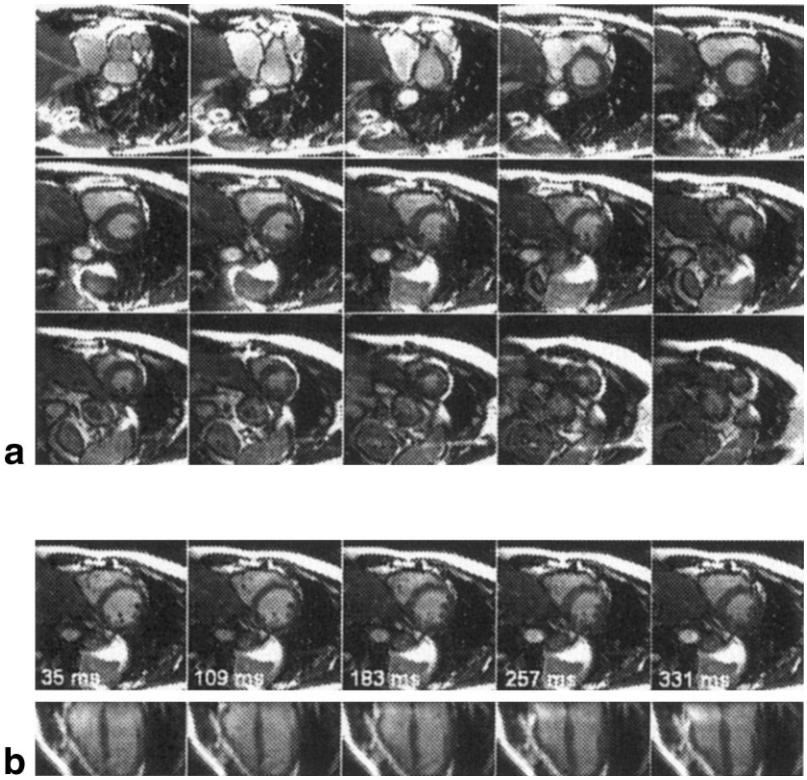

FIG. 8. Cine 3D single breathhold dataset obtained with 5× *k-t* BLAST and 65% partial Fourier sampling in a patient. The central 15 slices are shown for the end-systolic phase (**a**). Selected time frames showing both short-axis and reformatted four-chamber view plane (**b**) (20 timeframes were sampled every 37 ms in a single breathhold of 18 sec).

addition of another spatial dimension, as with the 3D acquisition in this work, substantially increases the size of *x-f* space for signal packing. Thus, the extension to 3D alleviates the problem from increased signal packing due to a smaller number of time cardiac phases in cardiac-gated acquisitions. As with all reduced acquisition methods, the reconstructed image is an approximation of the true image. Therefore, even though *k-t* BLAST allows a better approximation of the true image than previous methods, it may not recover all the information provided by a fully sampled dataset. The inability to completely recover missing data is manifested as reconstruction error (see Figs. 4, 5). The present study found that for 3D cardiac-gated cine acquisitions the unrecovered information at 5-fold acceleration was generally minor. The reconstructed images were of good quality, and *k-t* BLAST achieved lower reconstruction error than conventional methods such as sliding window reconstruction. It was furthermore demonstrated that contour areas extracted from *k-t* BLAST scans and conventional, fully sampled slices are comparable.

Using the current scanner implementation of *k-t* BLAST, it was possible to acquire volumetric datasets of the heart at high spatial ($2 \times 2 \times 5$ mm^3) resolution with temporal frames acquired every 28–37 ms in a single breathhold lasting 20–22 sec (for a heart rate of 55–80 beats/min), with the training data being obtained separately. The acquisition strategy was well tolerated by healthy subjects and patients. In general, 3D acquisitions are preferable for imaging the heart to avoid misregistration problems possible in multislice, multibreathhold acquisitions. In addition, the transient signal behavior of flowing blood is improved in 3D SSFP due to thick-slab excitation. Volume excitation has also been shown to provide better blood-myocardial contrast when compared to 2D acquisition of the heart (4). In this work, however, a flip angle smaller than the angle for optimal blood-cardiac tissue contrast had to be used due to specific absorption rate (SAR) limitations. This slightly counteracted the gain in CNR from 3D imaging. Future implementation will incorporate flip angle weighting to address SAR related limitations (16).

The modified profile order proved efficient in reducing eddy current-related image artifacts arising from the large phase-encode steps associated with sparse sampling. Residual artifacts are considered to be related to the varying number of dummy cycles at the end of each cardiac cycle, depending on the R-R interval.

Inconsistency of the acquisitions of low-resolution training data and undersampled, high-resolution data, when acquired in separate breathholds, may lead to reconstruction errors. These errors can be shown to be negligible for shifts within 5% of the FOV. Given a mean positional difference of 3.4 ± 2.9 mm between the two consecutive breathholds employed in the split acquisitions, image degradation can be assumed to be small. The insensitivity of the reconstruction to small positional shifts between the undersampled, high-resolution and the low-resolution training data is related to the very low spatial resolution ($2 \times 23 \times 11$ mm^3) in the training data. In future work, higher acceleration factors will be investigated, potentially allowing interleaved acquisition of undersampled data and training data in a breathhold of less than 18 sec.

In conclusion, *k-t* BLAST is a promising strategy to speed up cine 3D imaging of the heart, allowing for whole-heart coverage in a single breathhold at both high spatial and temporal resolutions. Such an approach holds consid-

erable potential for rapid assessment of cardiac function and anatomy, allowing for minimal examination time with increased patient comfort and throughput.

REFERENCES

1. Barkhausen J, Ruehm SG, Goyen M, Buck T, Laub G, Debatin JF. MR evaluation of ventricular function: true fast imaging with steady-state precession versus fast low-angle shot cine MR imaging: feasibility study. Radiology 2001;219:264–269.
2. Li W, Stern JS, Mai VM, Pierchala LN, Edelman RR, Prasad PV. MR assessment of left ventricular function: quantitative comparison of fast imaging employing steady-state acquisition (FIESTA) with fast gradient echo cine technique. J Magn Reson Imag 2002;16:559–564.
3. Plein S, Bloomer TN, Ridgway JP, Jones TR, Bainbridge GJ, Sivananthan MU. Steady-state free precession magnetic resonance imaging of the heart: comparison with segmented *k*-space gradient-echo imaging. J Magn Reson Imag 2001;14:230–236.
4. Jung BA, Hennig J, Scheffler K. Single-breathhold 3D-true FISP cine cardiac imaging. Magn Reson Med 2002;48:921–925.
5. Setser RM, Fischer SE, Lorenz CH. Quantification of left ventricular function with magnetic resonance images acquired in real time. J Magn Reson Imag 2000;12:430–438.
6. Pruessmann KP, Weiger M, Scheidegger MB, Boesiger P. SENSE: sensitivity encoding for fast MRI. Magn Reson Med 1999;42:952–962.
7. Madore B, Glover GH, Pelc NJ. Unaliasing by Fourier-encoding the overlaps using the temporal dimension (UNFOLD), applied to cardiac imaging and fMRI. Magn Reson Med 1999;42:813–828.
8. Kellman P, Epstein FH, McVeigh ER. Adaptive sensitivity encoding incorporating temporal filtering (TSENSE). Magn Reson Med 2001;45:846–852.
9. Tsao J. On the UNFOLD method. Magn Reson Med 2002;47:202–207.
10. Tsao J, Behnia B, Webb AG. Unifying linear prior-information-driven methods for accelerated image acquisition. Magn Reson Med 2001;46:652–660.
11. Tsao J, Boesiger P, Pruessmann KP. *k-t* BLAST and *k-t* SENSE: dynamic MRI with high frame rate exploiting spatiotemporal correlations. Magn Reson Med 2003;50:1031–1042.
12. McKenzie CA, Ohliger MA, Yeh EN, Price MD, Sodickson DK. Coil-by-coil image reconstruction with SMASH. Magn Reson Med 2001;46:619–623.
13. Fischer SE, Wickline SA, Lorenz CH. Novel real-time R-wave detection algorithm based on the vectorcardiogram for accurate gated magnetic resonance acquisitions. Magn Reson Med 1999;42:361–370.
14. McConnell MV, Khasgiwala VC, Savord BJ, Chen MH, Chuang ML, Edelman RR, Manning WJ. Prospective adaptive navigator correction for breath-hold MR coronary angiography. Magn Reson Med 1997;37:148–152.
15. Riederer SJ, Tasciyan T, Farzaneh F, Lee JN, Wright RC, Herfkens RJ. MR fluoroscopy: technical feasibility. Magn Reson Med 1988;8:1–15.
16. Schaeffter T, Weiss S, Boernert P. A SAR-reduced steady state free precessing (SSFP) acquisition. In: Proc 10th Annual Meeting ISMRM, Honolulu, 2002. p 2351.